Published in "Advanced photonics with second-order nonlinear processes", ed. A. Boardman pp. 89-112 (Kluver Academic, Dordreht, The Netherlands,1999).

# CONTROL OF LASER LIGHT PARAMETERS BY $\chi^{(2)}:\chi^{(2)}$ NONLINEAR OPTICAL DEVICES

S. SALTIEL, I. BUCHVAROV, K. KOYNOV
*University of Sofia, Faculty of Physics,*
*Quantum Electronics Department,*
*5 J. Bourchier Blvd., 1164 Sofia, Bulgaria*

**Abstract**

Nonlinear optical devices based on cascaded second order processes ($\chi^{(2)}:\chi^{(2)}$ cascading) able to control laser light parameters are reviewed. Such parameters of the laser light as phase, intensity, polarization and pulse duration are considered. Special attention is paid to cascaded $\chi^{(2)}$ nonlinear optical devices suitable for mode-locking and intracavity pulse control. Theoretical approaches used to investigate these types of nonlinear optical devices are also reviewed.

## 1. Introduction

The possibility to use second order nonlinear optical processes to measure and control parameters of the laser light was noticed long time ago. First typical example is the measurement of laser pulse duration. The pulse duration can be recalculated from intensity autocorrelation function obtained with autocorrelator based on second harmonic generation (SHG) [1-3]. For measuring frequency chirp of the pulse was developed interferometric autocorrelation technique [4,5]. For full characterisation of the measured pulses (duration, shape and frequency chirp) more sophisticated technique called FROG technique - frequency resolved optical gate [6-9] is now used.

Laser light polarization can also be controlled by nonlinear optical devices based on second order processes. In [10,11] is shown that crystal for second harmonic generation can be used for measurement of the polarization extinction coefficient of laser light. This method is especially suitable for measurement very small extincion coefficients ($10^{-5}$-$10^{-8}$).

In the late 1980s and during 1990s a number of different experiments demonstrated that a second order nonlinear optical device called nonlinear mirror [12] can be used as a mode-locking device [13-17] and for intracavity pulse control [18-20]. This nonlinear mirror is constructed from a SHG crystal and dichroic mirror. At this early stage for explanation of the principle of operation of the nonlinear mirror single quadratic processes were used. At present, when we have much more understanding on cascaded second order processes can be shown that $\chi^{(2)}:\chi^{(2)}$ cascading as we will discuss in this review can play important role in the mode-locking properties of the nonlinear mirror as well.

Rediscovering of cascaded processes in 1992 [21-25] opened new frontiers for development of $\chi^{(2)}$ nonlinear optical devices. $\chi^{(2)}:\chi^{(2)}$ cascading can be used successfully for the control of the phase of the fundamental beams involved in different types second order processes [26-31]. From the other hand generation of the nonlinear phase shift (NPS) can be the base for construction of nonlinear optical devices with intensity dependent transmission [32-34] or with possibilities to control the polarization of the transmitted light [35-36]. Pulse compression and mode-locking can also be realized with nonlinear optical devices based on cascaded second order processes [17,36].

The idea of cascaded second order processes was for the first time investigated with respect to the exploration the possibility to generate third harmonic in single quadratic crystal [37-39].

Let us consider single $\chi^{(2)}$ media with fundamental input wave $E(\omega) = a_{10}\exp(i\varphi)$ at frequency $\omega$ (fig. 1).

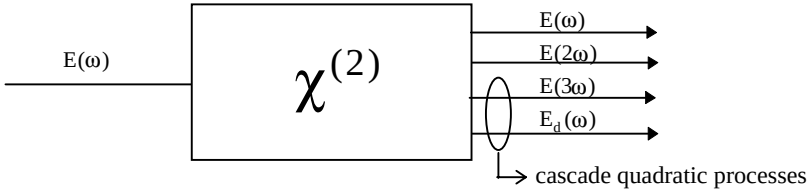


*Figure 1*. Cascade processes in single $\chi^{(2)}$ media.

Nonlinear polarization at frequency $2\omega$ is a source for generation of second harmonic wave $E(2\omega)$

$$E(2\omega) \propto d_{\text{eff}}^{(2)} E(\omega)E(\omega). \qquad (1)$$

Second harmonic wave (SHW) and the fundamental wave (FW) create also polarization at frequency $3\omega$, that becomes a source for generation of third harmonic wave $E(3\omega)$

$$E(3\omega) \propto d_{eff}^{(2)} E(\omega) E(2\omega) \tag{2}$$

and as a result

$$E(2\omega) \propto \frac{d_{eff}^{(2)} d_{eff}^{(2)}}{\Delta k} \left(E(\omega)\right)^3. \tag{3}$$

The term $\frac{d_{eff}^{(2)} d_{eff}^{(2)}}{\Delta k}$ is in fact "effective" cascade third order nonlinearity $\chi_{casc}^{(3)}$ responsible for the process of third harmonic generation in single quadratic media. The magnitude of the $\chi_{casc}^{(3)}$ can be bigger or smaller than the intrinsing cubic nonlinearity $\chi_{int}^{(3)}$, depending on the magnitude of the phase mismatch $\Delta k$ for the step that is nonphase matched. Usually one of the two steps ($\omega + \omega = 2\omega$ or $2\omega + \omega = 3\omega$) is phase matched and the other is not phase matched. It is impossible using the natural birefegence of the crystal to achieve simultaneous phase matching for both second-order processes. Only recently it was shown that using quasi phase matched technique it is possible to phase match both $\chi^{(2)}$ steps simultaneously [40].

Single crystal third harmonic generation was used as a standard source for $\chi^{(3)}$ measurement [38-39]. Note that $\chi_{casc}^{(3)}$ is in most of the cases positive, so can be used for absolute measurement of the sign of natural $\chi^{(3)}$.

**2. Control of laser light phase**

Totally different result we have when another consequence of $\chi^{(2)}$ processes $\omega + \omega = 2\omega \rightarrow 2\omega - \omega = \omega$ is considered.

First step is the same - generation of SHW $E(2\omega)$ (fig.2,a). The second step is downconversion of generated SHW (fig. 2, b). As a result downconverted FW $E_d(\omega)$ at fundamental frequency $\omega$ is generated

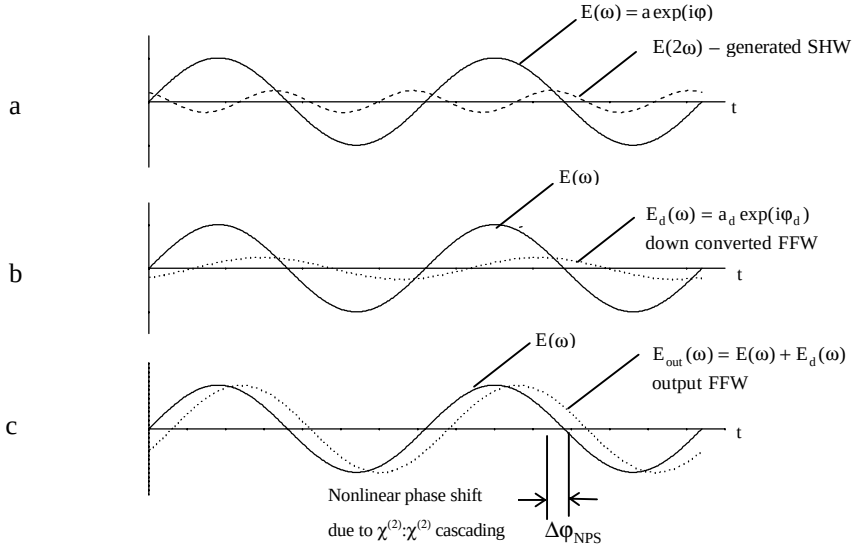


Figure 2. Simplified physical explanation of the process of phase shifting via $\chi^{(2)}:\chi^{(2)}$ cascading.

$$E_d(\omega) \propto d_{eff}^{(2)} E(\omega) E(2\omega) \tag{4}$$

or

$$E_d(\omega) \propto \frac{d_{eff}^{(2)} d_{eff}^{(2)}}{\Delta k} \left(E(\omega)\right)^3. \tag{5}$$

If the process of SHG is slightly mismatched ($\Delta k \neq 0$) then the local phase of $E_d(\omega)$ is different from the phase of the FW. The two waves $E(\omega)$ and $E_d(\omega)$ interfere at the output of the crystal and as a result the output FW obtains NPS with magnitude that depends on the input intensity (fig. 2,c). The higher is the input intensity the higher is the nonlinear phase shift. This process is in fact self phase modulation due to $\chi^{(2)}$ processes and is observed when SHG process is with Type I interaction. As we will see later the effect of cross phase modulation can be obtained with SHG Type II or sum frequency generation. Additional degree of control of the NPS can be realized when one uses seeded SHG [23] or two pass phase shifting devices [41].

2.1. PHASE SHIFTING WITH TYPE I SHG.

Typical dependencies of the NPS and the fundamental depletion as a function of the distance, mismatch and the input intensity are shown on figures 3-5. The dependence of

the NPS on the input amplitude and the distance has stepwise behaviour. The middle of each plato corresponds to the point of full reconstruction of the amplitude of the FW. At the same point the SHW has its minimum. Each step corresponds to the nonlinear phase jump equal to $\pi/2$ or less depending on the magnitude of the phase mismatch $\Delta kL$. The dependence of the NPS as a function of the mismatch $\Delta kL$ has dispersion like shape. NPS is zero for exact phase matching, $\Delta kL$=0, and is decreasing asymptotically to zero for big values of $\Delta kL$.

For low values of input amplitude the process of NPS is described by the formulae obtained with fixed intensity approximation [42]. Suggesting $\sigma a_{10} << \Delta k$

$$\Delta\varphi_{NPS} = \frac{\sigma^2 a_{10}^2}{\Delta k^2}\left[\Delta kL - \sin(\Delta kL)\right]. \quad (6)$$

For $\Delta kL = \pi$, where is the maximum of the NPS & $\Delta kL$ dependence

$$\Delta\varphi_{NPS} = \frac{1}{\pi}\sigma^2 a_{10}^2 L^2 = \frac{1}{\pi}\frac{L^2}{L_{NL}^2}. \quad (7)$$

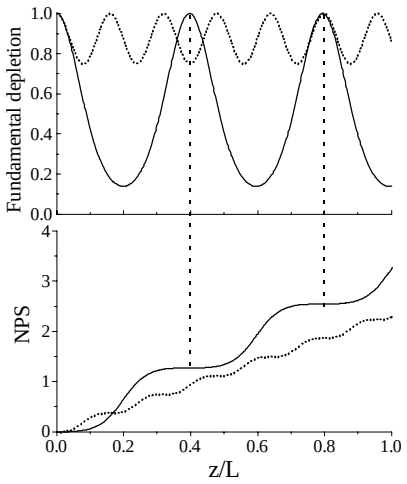


*Figure 3.* Nonlinear phase shift and fundamental depletion versus normalized distance z/L. Normalized input intensity is $\sigma a_{10} L = 10$. Normalized mismatch $\Delta kL$ is 3 (solid line) and 30 (dotted line)

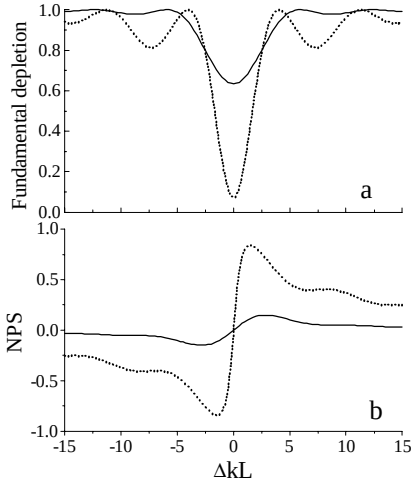


*Figure 4.* Fundamental depletion (a) and nonlinear phase shift (b) versus normalized mismatch $\Delta kL$. Normalized input intensity $\sigma a_{10} L$ is 0.7 (solid line) and 2 (dotted line).

In this limit is possible to introduce $n_{2,casc}$ but this analogy will be valid only for low input intensities ($L_{NL} >> L$)

$$n = n_o + n_{2,casc} a_{10}^2 + n_2 a_{10}^2, \quad (8)$$

where $n_{2,casc} = \frac{\lambda\sigma^2}{2\pi^2} L$. In this limit $n_{2,casc} > n_2$ [21].

For higher input intensities is impossible to introduce $n_{2,casc}$, that is due to $\chi^{(2)}:\chi^{(2)}$ cascading. For these intensities $L_{NL} < L$

$$n = n_o + n_{1,casc} a_{10} + n_2 a_{10}^2. \quad (9)$$

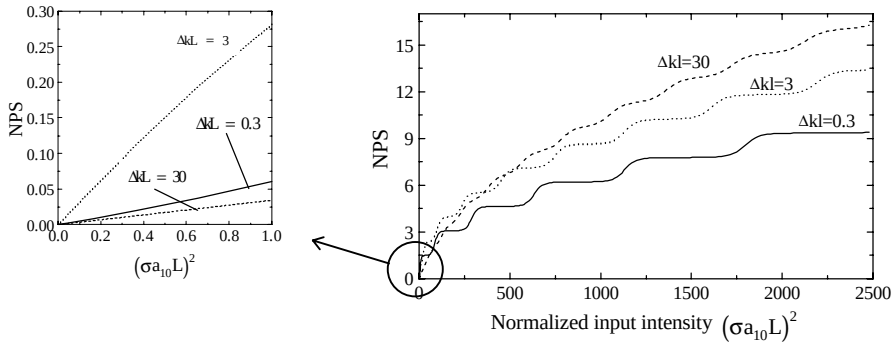


*Figure 5*. Nonlinear phase shift as a function of the input intensity. Left the case of $L/L_{NL} < 1$. Right - the case of $L/L_{NL} >> 1$.

Our group [43] has shown that using $\chi^{(3)}:\chi^{(3)}$ cascading in centrosym-metric media is possible to simulate the behaviour of the inherent $n_2$. In this case at high input intensities $\Delta\varphi_{NLS}$ has linear dependence on the intensity and the distance after averaging over the steps.

In the case of nonzero input signal at $2\omega$ the nonlinear phase shift of the fundamental wave depends on the input relative phase difference $\Delta\varphi_0 = 2\varphi_1 - \varphi_2$ between the phases of the FW and SHW. As it is seen from Fig. 6 the presence of seeding

allows for obtaining NPS of the fundamental waves at exact phase matching condition ($\Delta k = 0$). In this case the change of the magnitude of the shift can be controlled not only by the amplitude of the pump FW but also by the input phase of the seeded SHW wave. In the approximation of negligible fundamental depletion when $\Delta k = 0$ we have for the NPS of the FW [30]:

$$\Delta\varphi_{NPS}(L) = -\sigma_1 \frac{a_{30}a_{20}}{a_{10}} L\cos(\Delta\varphi_0). \qquad (10)$$

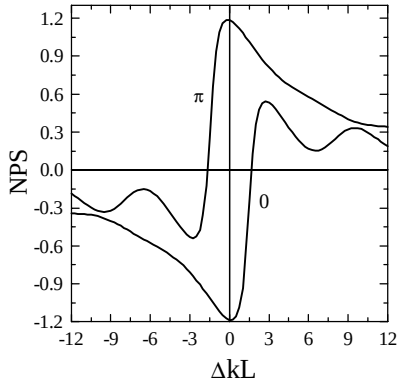


*Figure 6.* Nonlinear phase shift as a function of the wavevector mismatch $\Delta kL$ for two different values of the input phase difference. Normalized input amplitude is $\sigma a_{10}L=2$.

The induced phase shift in this case is due to the single second order process. The sign of the shift depends on the sign of the second order susceptibility tensor and the magnitude of $\Delta\varphi_0$. The analysis of the "seeding case" is important for understanding the phase shifting properties of two pass devices as nonlinear mirror.

## 2.2. CROSS PHASE MODULATION WITH TYPE II SHG.

In the case of type II SHG the input waves are respectively ordinary and extraordinary wave for the nonlinear birefrigent media (fig. 7). Nonlinear interaction of this two waves under phase matched condition $\Delta k = k_{2e} - k_{1o} - k_{1e} = 0$ leads to generation of extraordinary SHW.

For maximum conversion efficiency the amplitudes of the two input waves must be equal. Type II with equal amplitudes at the input is practically equivalent to Type I SHG. From point of view to obtain large NPS more interesting is the case of nondegenerate Type II SHG ($A_{1o} \neq A_{1e}$). In this case the weaker wave has stronger NPS and the amount of the NPS of the weaker wave is defined by the amplitude of the stronger wave.

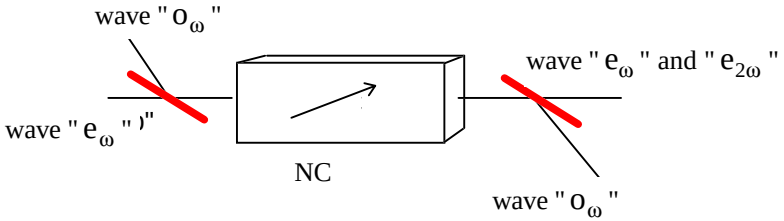


*Figure 7.* Type II SHG in negative uniaxial quadratic nonlinear crystal.

This statement can be easily illustrated by simple mathematical analysis of the system of equations (11) that describes Type II SHG:

$$\begin{aligned}
\frac{dA_{1o}}{dz} &= -i\sigma_1 A_2 A_{1e}^* \exp(-i\Delta kz),\\
\frac{dA_{1e}}{dz} &= -i\sigma_1 A_2 A_{10}^* \exp(-i\Delta kz), \qquad (11)\\
\frac{dA_2}{dz} &= -i\sigma_2 A_{1o} A_{1e} \exp(i\Delta kz),
\end{aligned}$$

where $\sigma_i$ are the nonlinear coupling coefficients.

Using fixed intensity approximation that is valid for low input intensities expressions for the NPS of the two FW can be obtained [30,31]

$$\Delta\varphi_{1o} = \sigma_2\sigma_1 a_{1e}^2 L^2 \frac{(\Delta kL)}{(\Lambda L)^2}\left[1 - \operatorname{sinc}(\Lambda L)\right], \qquad (12.1)$$

$$\Delta\varphi_{1e} = \sigma_2\sigma_1 a_{1o}^2 L^2 \frac{(\Delta kL)}{(\Lambda L)^2}\left[1 - \operatorname{sinc}(\Lambda L)\right], \qquad (12.2)$$

where $\Lambda = \sqrt{\Delta k^2 + \sigma_2(\sigma_{10}a_{1e}^2 + \sigma_{1e}a_{1o}^2)}$.

It is seen that the nonlinear phase shift of the "o" wave is defined by the intensity $a_{1e}^2$ of the "e" wave and the NPS of the "e" wave is defined by the intensity $a_{1o}^2$ of the "o" wave. Another important feature of this cross phase modulation process is the fact that the obtained by the fundamental waves NPS does not depend on the relative phase difference between them at the input of nonlinear media.

On fig. 8 is shown NPS of the weaker and the stronger waves as a function of normalized input amplitude $\sigma aL$ of the stronger fundamental wave. The amount of the

phase jump between two neighbour steps is twice more than for the case of Type I SHG and degenerate Type II SHG ($r=1$) and for small values of $\Delta kL$ is close to $\pi$. The parameter $r$ is the ratio of the input intensities of the two fundamental waves. This ratio can be changed with varying the angle $\alpha$ between the polarization plane of single input FW and normal to the main plain of the crystal ($\vec{k},\vec{z}$ plane).

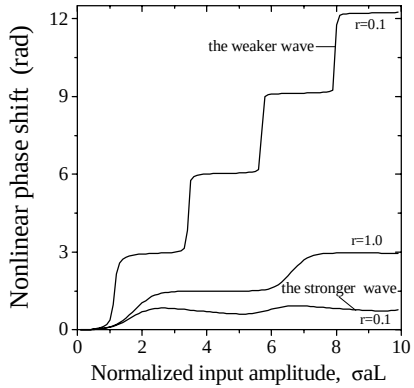


*Figure 8.* Nonlinear phase shift of the fundamental waves involved in Type II SHG. Normalized mismatch is $\Delta kL = 0.3$. As a parameter is indicated the ratio of the input intensities.

On fig. 9 is presented the amount of NPS collected by the both waves at the

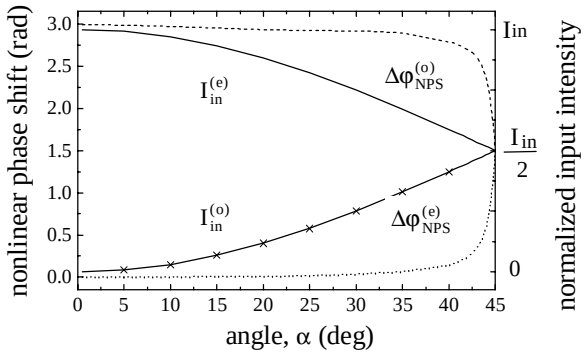


*Figure 9.* Input intensities (solid line) and NPS (dotted line) of the ordinary and extraordinary wave as a function of angle $\alpha$ (see the text). Normalized mismatch is $\Delta kL = 0.3$.

point of first full reconstruction as a function of the angle $\alpha$. From the figure is seen that small disbalance of the input intensities of the fundamental waves leads to big difference of NPS obtained by them. This fact as we show later can be used for obtaining intensity dependent polarization rotation [36].

## 2.3. NONLINEAR FREQUENCY DOUBLING MIRROR AS A DOUBLE PASS PHASE SHIFTING ELEMENT

Nonlinear frequency doubling mirror (NFDM) shown on fig. 10 was initially known as a device with intensity dependent reflection [12]. As a rule for obtaining intensity dependent reflection with this device is necessary (I) frequency doubling crystal to be at exact phase matched condition and (ii) the mirror M to have maximum reflection at second harmonic frequency and partial reflection at fundamental frequency.

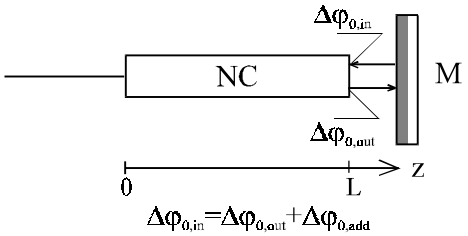


*Figure 10.* Nonlinear frequency doubling mirror. NC - crystal for SHG, M - mirror, $\Delta\varphi_0 = 2\varphi_1 - \varphi_2$.

Recently [41] we have shown that this device, when tuned not exactly but near exact phase matching can be efficient phase shifting element. By proper choosing the distance between the crystal and the mirror one can always obtains 100% reflection of the NFDM. However, in contrast to original "Stankov" type nonlinear mirror, the back reflector of the NFDM for phase shifting should have maximum reflection for both waves - fundamental and second harmonic. On fig. 11 is shown the dependence of the intensity reflection and the nonlinear phase shift as a function of the linear phase difference $\Delta\varphi_{add}$, that depends on the mirror - crystal distance.

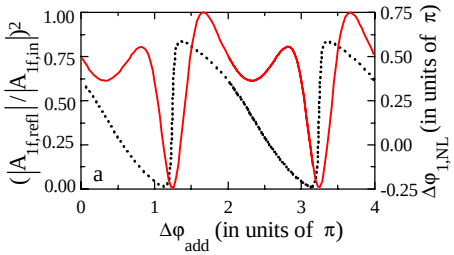


*Figure 11.* NPS and intensity of the reflected fundamental wave versus linear phase difference $\Delta\varphi_{add}$ for the case of Type I SHG ($\sigma a_{1o}L=2$, $\Delta kL=1$).

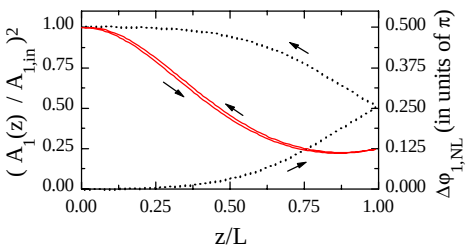


*Figure 12.* Intensity (solid line) and the NPS (dotted line) of the fundamental wave inside the crystal: on the way to and back from the back reflector $\sigma a_{1o}L=2$, $\Delta kL=1$, $\Delta\varphi_{add} = 1.67\pi$).

It is seen that by proper tuning of $\Delta\varphi_{add}$ both 100% reflection and large NPS can be obtained. On fig. 12 is shown the dynamic of the NPS collection and the reconstruction of fundamental intensity during the two pass of the fundamental wave through the crystal for proper chose $\Delta\varphi_{add}$.

NFDM is two to four times more efficient phase shifting element than single pass second harmonic crystals. It can be used as an element for all optical switching devices [41] and for mode-locking [17] of pulsed and CW lasers.

### 2.4. ENHANCED NPS VIA MULTISTEP $\chi^{(2)}$ CASCADING

Another way to improve phase shifting efficiency due to cascade processes is to increase the number of the second order processes in which the fundamental wave is involved. Up to now only consequence of the two processes was investigated.

$$\omega + \omega = 2\omega \rightarrow 2\omega - \omega = \omega .$$

Only recently in [44] was considered the more complicate case when in the crystal are possible two processes: SHG and third harmonic generation and both of them are simultaneously near phase matched (fig.13).

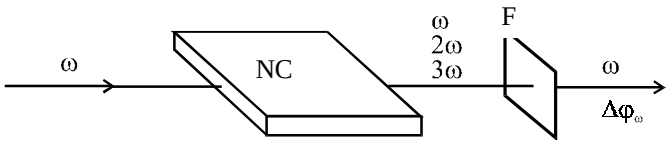


*Figure 13.* The idea of multistep $\chi^{(2)}$ cascading. NC - nonlinear crystal, F - harmonic stop.

The process of SHG is taken to be Type I. Then following second order processes must be considered for analysing NPS collected by the fundamental wave.

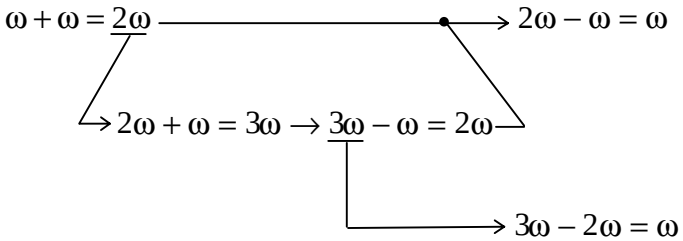


We see that two, three and four step $\chi^{(2)}$ cascading contribute to the process of reconverting depleted fundamental wave yelding this way large NPS.

On fig. 14 is compared NPS efficiency for two and multistep cascading. With multiistep cascading almost four times less input intensity is necessary for obtaining NPS with amount of $\pi$. This more efficient way to generate large NPS can be used for reduction of the switching intensity of existing all optical switching devices based on $\chi^{(2)}:\chi^{(2)}$ cascading and for construction intracavity nonlinear optical devices for mode-locking and pulse duration control.

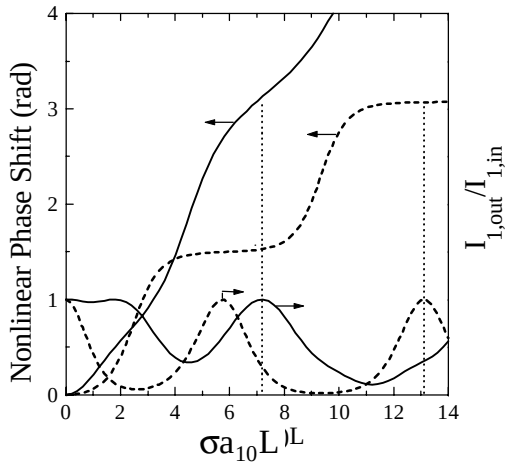


*Figure 14.* NPS and fundamental throughput as a function of input amplitude $\sigma a_{10}L$ for SHG Type I only (dashed line), $\Delta k_2 L = 0.3$ and simultaneous SHG and THG (solid line) $\Delta k_2 L = 4.8$, $\Delta k_3 L = 30$ ($\Delta k_2 = k_2 - 2k_1$; $\Delta k_3 = k_3 - k_2 - k_1$)

## 3. Polarization Rotation as a Result of Cascaded Processes

Polarized light entering the birefrigent crystal splits into two waves: ordinary wave with polarization plane perpendicular to the main plane of the crystal and extraordinary wave with polarization plane parallel to the main plain of the crystal. If ordinary and extraordinary waves obtain different nonlinear shift than at the output of the crystal will be observed change of the polarization state of the input light. Since NPS is intensity dependent then the change of polarization state will be also intensity dependent.

Intensity dependent change of polariztion state can be realised by exploring $\chi^{(2)}:\chi^{(2)}$ cascading during Type I [34] or Type II [35,36] process of SHG (fig. 15).

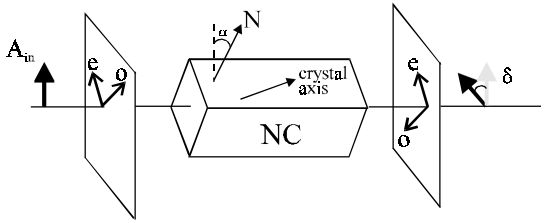


*Figure 15*. Main idea of polarization rotation due to quadratic cascading. NC - nonlinear crystal, N - normal to the plane formed by wavevector **k** and crystal axis, $\alpha$ - angle between input polarization and normal N, $\delta$ - angle of rotation of output polarization.

In the case of Type I SHG only the wave "o" collects NPS. If its value is $\pi$ the polarization is rotated by 90 degree. By definition, for small $\Delta kL$, we have full reconstruction of the amplitude of the fundamental wave for values for NPS equals to $\pi/2$, $\pi$, $3\pi/2$, ... This means that at this points we will have respectively, circular polarized light, linearly polarized light, again circular polarized light, ..... The intensity induced phase difference is:

$$\Gamma_{NPS} = \Delta\varphi^{(o)}_{NPS} \ .$$

In the case of type II SHG one of the waves, that is weaker, for example, "o" wave, collects NPS more than "e" wave. If the difference ["o" NPS - "e" NPS ] is $\pi$ the polarization is rotated by 90 degree. The advantage of Type II is that the first point of full reconstruction corresponds to NPS equals to $\pi$. The intensity induced phase difference is:

$$\Gamma_{NPS} = \Delta\varphi^{(o)}_{NPS} - \Delta\varphi^{(e)}_{NPS} \approx \Delta\varphi^{(o)}_{NPS} .$$

It is possible to improve twice the efficiency of polarization rotation in case of Type I SHG by use of two crystal in a row (fig. 16). The axes of the two crystals are in perpendicular planes. Let us consider the input polarization as a sum of two linearly polarized wave with perpendicular polarization vectors. In the first crystal named A the wave "a" is ordinary wave and collects NPS. In the second crystal named B the wave "b" is ordinary wave and collects also NPS, but with opposite sign. This way the intensity induced phase difference between the two waves is doubled. Respectively, the intensity for 90 degree rotation is twice less [34].

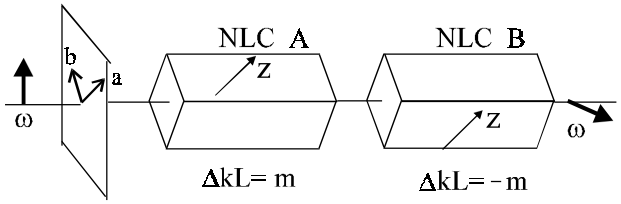


*Figure 16.* Two crystal scheme for polarization rotation.

Both schemes: two crystal scheme with Type I interaction and $\alpha = 45^o$ and one crystal scheme with Type II interaction and $\alpha = 40^o - 43^o$ give similar results. Since nonlinear intensity dependent phase difference $\Gamma_{NPS}$ is close to $\pi$ at the first point of the full reconstruction of the fundamental wave at the output of the crystal, the output wave remains predominantly linearly polarized. This is illustrated on fig. 17.

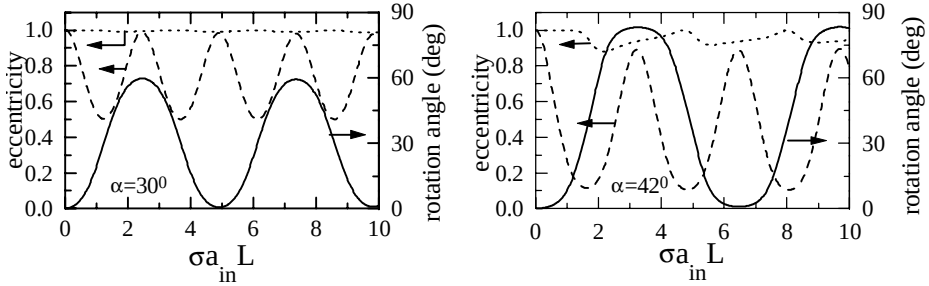


*Figure 17*. The eccentricity (dotted line), the rotation angle $\delta$ (solid line) and the square of the big axis, $a^2$, (dashed line) as a function of the normalized input intensity for two different input angles $\alpha$. The normalized phase mismatch $\Delta kL = 0.3$.

**4. Nonlinear Frequency Doubling Polarization Interferometer (NFDPI)**

The effect of intensity induced polarization rotation can be used for construction of so called nonlinear frequency doubling polarization interferometer [34,36]. The scheme of the interferometer is shown on fig. 18. It consists polarizer, frequency doubling crystal(s), phase corrector and analyzer. The phase corrector is used to compensate the different linear phase shift that the two waves obtain in the crystal.

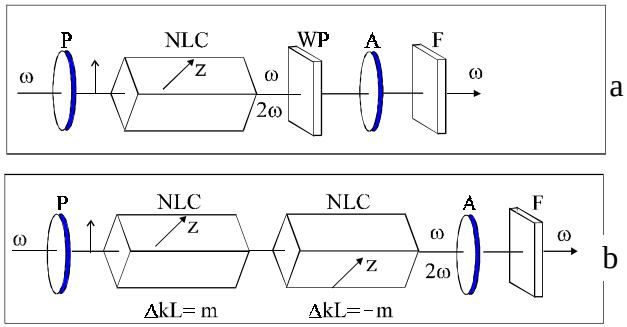


*Figure 18.* Nonlinear frequency doubling polarizatoin interferometer: a) single crystal scheme (with Type II SHG); b) double crystal scheme (with Type I SHG).

Depending on the mutual orientation of the polarizer and the analyser NFDPI exhibits self induced transparency or self induced darkening. The throughput of the NFDPI shown on fig. 18a is presented on fig.19. This device has also the capability to shorten input pulses. When the polarizer and the analyser are crossed strong shortening of the pulses can be obtained (fig. 20).

It is clear that the two capabilities of the NFDPI: pulse shortening and self induced transparency effect at relatively low power (we calculate 60 MW/cm$^2$ for 10 mm long KTP crystal) make this device suitable for mode locking of lasers with ring resonators. Another possible application may be all optical switching and sensor protection.

Experimentally NFDPI has been realised with bulk phase matched KTP [35] and with periodically poled $LiNbO_3$ [45].

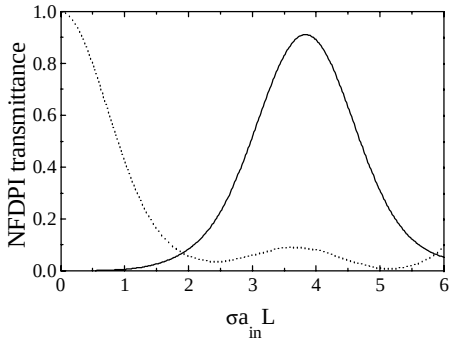


*Figure 19.* Fundamental throughput for parallel (dotted line) and crossed (solid line) polarizer and analyser for the single crystal NFDPI shown on fig. 18a. Input angle is $\alpha = 40^o$. Normalized mismatch $\Delta kL = 0.3$.

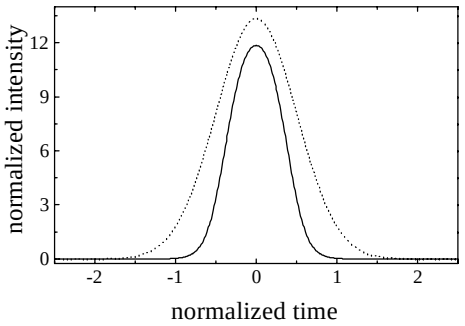


*Figure 20.* Single pass shortening of Gaussian pulse with the NFDPI shown on fig. 18a. Dashed line - input pulse, solid line - transmitted pulse. Input angle is $\alpha = 40^o$. Normalized mismatch $\Delta kL = 0.3$.

## 5. Role of $\chi^{(2)}$ Cascade Processes on the Performance of NFDM as a Mode-Locker

### 5.1. NFDM WITH TYPE I SHG CRYSTAL

In all of the experiments [14,15,17-20,46] ( with exception of [17] ) where nonlinear frequency doubling mirror with Type I SHG crystal has been used as a mode locker, the mode-locking effect is explained with the intensity dependent reflection of the NFDM. It was assumed that the phase mismatch $\Delta k = 0$ and that $\Delta\varphi_{add}$ (defined in part 2.3.) is equal to $\pi$. In the real experimental conditions, however, these two parameters had been tuned for obtaining best mode-locking and shortest generating pulses without taking care to measure its exact values. The difficulties arises from the facts (i) that the phase jumps of the fundamental and second harmonic waves at the back reflector are unknown and (ii) that intracavity SH intensity has its maximum when one achieves good mode locking and no care was taken to determine if this point corresponds to exact phase matching condition.

As we already discussed in part. 3 NFDM is an effective double pass phase shifter if the wavevector mismatch and the distance SH crystal - back reflector are properly chosen.

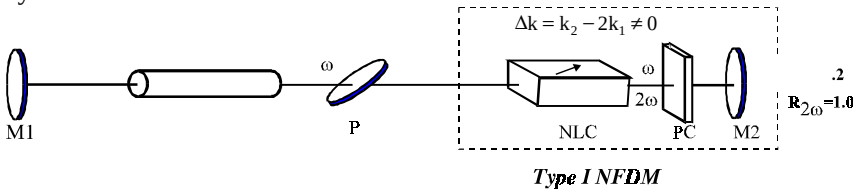


*Figure 21.* Typical set-up for mode - locking with nonphasematched NFDM with Type I SHG crystal

Here we investigate intensity reflection and NPS for typical experimental set up (fig. 21) for mode locking with NFDM with Type I SHG crystal. The process is considered to be with $\Delta kL = 3$ and $\Delta\varphi_{add}$ is taken to be $\pi$ - the value that is recommended when NFDM is used as an amplitude mode locker [12].

The results of the computer simulations are shown on fig. 22 for three different values of the linear reflection coefficient of the mirror M2: 20, 40 and 80%. The graphs show that the effect of intensity dependent increase of the reflection of the NFDM is accompanied by strong intensity dependent phase modulation of the fundamental wave. This means that NFDM when used as intracavity laser element should be considered as a nonlinear optical device with combined amplitude and phase passive mode locking effect. From fig. 22 is clearly seen that the higher is the linear reflection of M2, the higher is the phase modulation efficiency for one and the same input intensities.

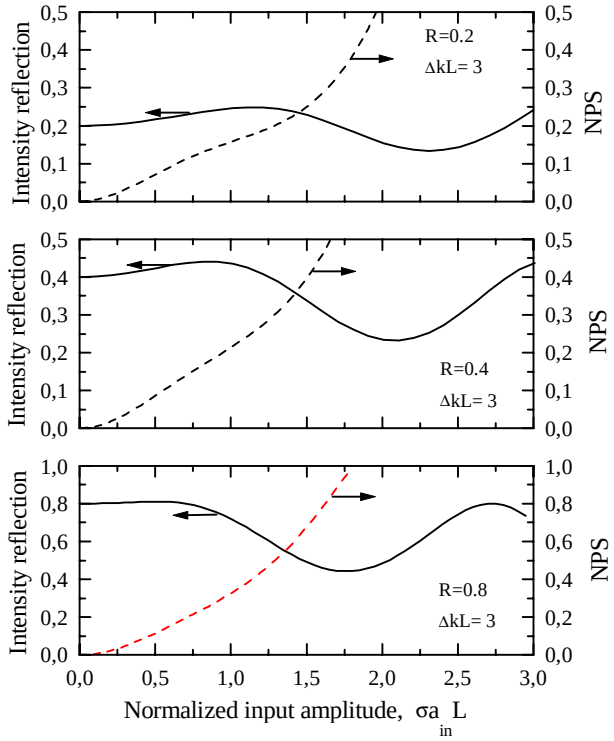


*Figure 22.* Intensity reflection (solid line) and nonlinear phase shift (dotted line) of the fundamental wave as a function of normalized input amplitude for three different values for reflection of the mirror M2.

The requirement of low linear reflection of M2 was one of the drawback for NFDM working at exact phase matching conditions since the small $R_{M2}$ leads to very high threshold for the laser. The fact that NFDM can work with high reflecting back mirror makes this device suitable for CW pumped lasers [15,17]. The presence of intracavity diaphragm can lead to effective Kerr lens mode locking as it was observed in [17].

## 5.2. NFDM WITH TYPE II SHG CRYSTAL

In almost half of the experimental works that use NFDM as a mode locker Type II SHG crystals [13,46,48-50] were used. In these works is accepted that this type NFDM has the same behaviour as NFDM with exactly phase matched Type I SHG crystal i.e. intensity dependent reflection coefficient. As we discussed in part 2.2 and part 3 $\chi^{(2)}$ cascade processes in Type II SHG crystal lead to stronger phase modulation of the fundamental wave and to polarization rotation. Analysis of the NFDM with Type II SHG crystal is not done by now. We present here some of our preliminary results.

Experimental set up of a laser mode-locked with the NFDM with Type II SHG crystal is shown on fig. 23. We will suggest that the intensities of the ordinary "o" and extraordinary "e" waves in SH crystal are slightly different, i.e. angle $\alpha$ is 40-42$^o$. M2 has maximum reflection for both second harmonic and fundamental wave.

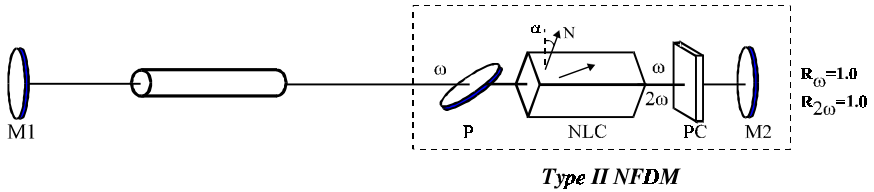


*Figure 23.* Type II NFDM as mode locker

Type II NFDM shown on fig. 23 is in some aspects similar to the nonlinear frequency doubling polarization interferometer [36] discussed in part 4 with this difference that in the case of NFDM the light passes twice through the crystal. Instead of self induced transparency in the case of NFDPI, in the case of Type II NFDM we should expect intensity dependent reflection coefficient. Due to the double pass geometry the intensity needed for maximum reflection will be less than intensity needed for maximum transmission of the scheme shown on fig. 18a. Additional advantage of the Type II NFDM is the possibility to change $\Delta\varphi_{add}$ by playing with mirror - crystal distance or inserting phase plates.

On fig. 24 are compared reflection coefficients of NFDM with a) Type II SHG crystal, $\Delta\varphi_{add} = \Delta\varphi_{in} - \Delta\varphi_{out} = 2\pi$, $\alpha = 40^o$, $\Delta kL = 0.3$ and b) Type I SHG crystal at exact phase matched condition [12]. It is clearly seen that Type II NFDM exhibits much stronger increase of reflection with increase of fundamental intensity in comparison with the conventional "Stankov" nonlinear mirror [12]. The physical explanation of the intensity dependent reflection of Type II NFDM is different. With the help of the phase corrector PC and by changing mirror-crystal distance linear reflection of the NFDM can be made to take any value from 0 to 1. Due to intensity induced rotation of the polarization (part 3 or [36]) Type II NFDM has intensity induced change of the reflection coefficient. Type II NFDM can be either positive or negative feedback for the laser depending of the chosen linear reflection coefficient of the NFDM as a whole.

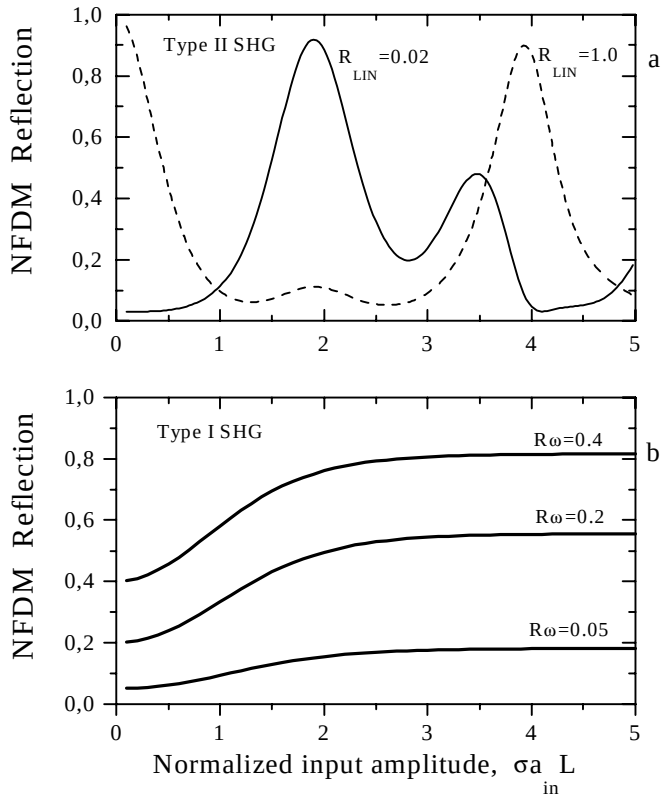


*Figure 24.* NFDM reflection as a function of normalized input amplitude for case of using Type II crystal for SHG (a) and Type I crystal for SHG (b) and different values of the reflection of mirror M2.

## 6. Approximate theoretical approaches for description of nonlinear optical devices based on $\chi^{(2)}:\chi^{(2)}$ cascading

In this part will be presented some approximate theoretical approaches used by us for investigation nonlinear optical devices based on $\chi^{(2)}:\chi^{(2)}$ cascading. Let us take as example Type I SHG process. Generalization for Type II SHG, sum frequency mixing and other second order processes is not difficult.

In the case of SHG Type I relevant equations are:

$$\frac{dA_1}{dz} = -i\sigma A_2 A_1^* \exp(-i\Delta kz) \ , \tag{13.1}$$

$$\frac{dA_2}{dz} = -i\sigma A_1 A_1 \exp(i\Delta kz) \ . \tag{13.2}$$

This system can be rewritten for the real amplitudes and phases of the interacting waves:

$$\frac{da_1}{dz} = \sigma a_2 a_1 \sin\Phi \, , \tag{14.1}$$

$$\frac{da_2}{dz} = -\sigma a_1^2 \sin\Phi \, , \tag{14.2}$$

$$\frac{d\varphi_1}{dz} = -\sigma a_2 \cos\Phi \, , \tag{14.3}$$

$$\frac{d\varphi_2}{dz} = -\sigma \frac{a_1^2}{a_2} \cos\Phi \, , \tag{14.4}$$

where $A_1 = a_1 \exp(i\varphi_1),\ A_2 = a_2 \exp(i\varphi_2),\ \Phi = \varphi_2 - 2\varphi_1 - \Delta kz$.
The system (14) has two important invariants

$$a_1^2 + a_2^2 = a_{10}^2 + a_{20}^2 = u^2, \tag{15}$$

$$\sigma a_1^2 a_2 \cos\Phi + \frac{\Delta k}{2} a_2^2 = \Gamma . \tag{16}$$

where $\Gamma = 0$ in the case of no seeding.

In general, possible approaches for solving exactly the system (2) are direct numerical integration of the relevant equations and analytical formulae expressed in Jacobi elliptic functions and integrals. Direct numerical integration is the most popular method for investigation of cascade processes. Big part of the results shown in this review are obtained this way. The use of analytical formulae expressed in Jacobi elliptic functions and integrals is rather difficult since the elliptic sinus and the elliptic integral of the third kind (used in the expressions for the NPS) have to be evaluated by complicated numerical calculations. There is a need for simple approximate approaches that allow to express and explain the phenomena based on $\chi^{(2)}$ cascading and to optimise nonlinear optical devices based on cascaded effects.

Following analytical approximations have been used by us:

a) fixed intensity approximation . Describes NPS only. Valid for low input intensities;

b) low depletion approximation (LDA). Describes fundamental depletion and NPS. Valid for $\sigma a_{in} < \frac{1}{2}\Delta k$;

c) high depletion approximation (HDA) - describes fundamental depletion and NPS at arbitrary input power intensities.

### 6.1. FIXED INTENSITY APPROXIMATION

Fixed intensity approximation was introduced for the first time for description NPS via Type I SHG [42]. Later fixed intensity approximation was extended for description of Type II SHG and sum frequency generation [30,31] and for description of NFDM as mode locker [17]. In comparison with the well known fixed amplitude approximation [37] in which both real amplitude and phase of the fundamental wave are considered constant, in the case of fixed intensity approximation only the fundamental amplitude is constant but $\varphi_1 = \varphi_1(z)$.

For the case of $a_{20} = 0$ with this approximation we have:

$$\left(\frac{a_2}{a_{10}}\right)^2 = a_{10}^2\left(\frac{\sigma}{Q}\right)^2 \sin^2(Qz), \tag{17}$$

where $Q^2 = 2\sigma^2 a_{10}^2 + \Delta k^2/4$. Then defining $\cos(\Phi)$ from (16) and integrating (14.3) following expression for the NPS of the fundamental wave can be obtained

$$\varphi_1 = \varphi_{10} + \Delta kL\left(\frac{\sigma a_{10}}{2Q}\right)^2 \left[1 - \operatorname{sinc}(2QL)\right]. \tag{18}$$

This approach correctly describes disperse like shape for the $\Delta k$ dependence of the NPS (fig. 4b) and also allows to define $n_{2,casc}$ (see (8)). However, does not describe the stepwise behaviour of NPS *versus* intensity dependence and does not describe fundamental depletion.

### 6.2. LOW DEPLETION APPROXIMATION - LDA

Expressing $\sin(\Phi)$ from (16) and substituting in (14.2) we obtain:

$$\frac{da_2^2}{dz} = -2\sigma u^3\sqrt{\left(\frac{a_2}{u}\right)^6 - \frac{Q^2}{2\sigma^2u^2}\left(\frac{a_2}{u}\right)^4 + \left(\frac{a_2}{u}\right)^2}. \tag{19}$$

For low conversion, $(a_2/u)^6$ term can be neglected and (19) can be integrated:

$$\left(\frac{a_2}{u}\right)^2 = 2M\sin^2(Qz); \qquad \left(\frac{a_1}{u}\right)^2 = 1 - 2M\sin^2(Qz), \tag{20}$$

where $M = \frac{1}{2}(\sigma u/Q)^2$, $\quad Q = \sqrt{2\sigma^2u^2 + \Delta k^2/4}$.

Then in case of Type I SHG with no seeding

$$\Delta\varphi_{NPS} = -\frac{\Delta kL}{2} + \frac{\Delta k}{2}\frac{\operatorname{arctg}\left[\sqrt{1-2M}\,\operatorname{tg}(QL)\right]}{Q\sqrt{1-2M}} \tag{21}$$

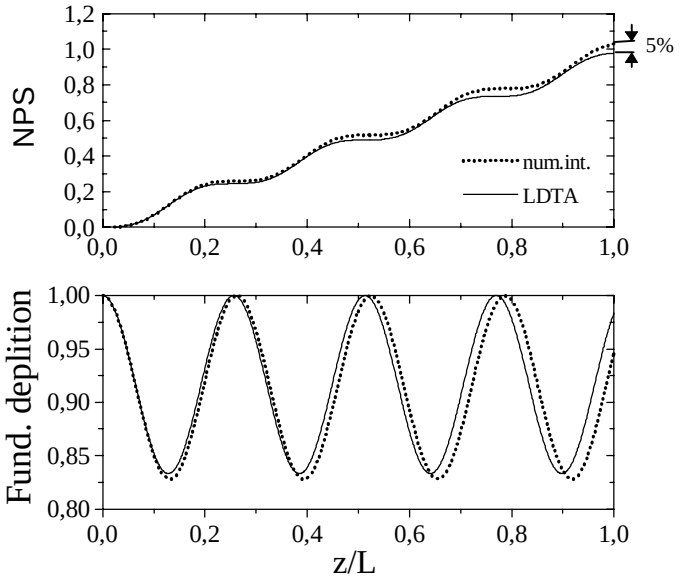


*Figure 25*. Comparison of exact numerical calculations (dotted line) and calculations with low depletion trigonometric approximation (solid line) for Type I SHG without seeding. $\Delta kL = 20$, $\sigma a_{10}L = 5$.

The range of validity of LDA was verified by comparison with exact numerical calculations (fig. 25). The depletion of the fundamental wave should not exceed 20%. In contrast to the fixed intensity approximation, LDA describes both the fundamental depletion and the stepwise behaviour of the NPS. LDA is suitable for description of mode locking devices based on cascaded second order processes. Similar formulae as (21) can be derived for the cases of presence of SH seeding and also for Type II SHG and sum frequency generation interactions.

6.3. HIGH DEPLETION APPROXIMATION - HDA

This approximation is valid practically for any fundamental depletion. The key idea is the replacement of the square of elliptic sinus in the expression for second harmonic intensity by:

$$\mathrm{sn}^2\left(\frac{z}{æ}|m\right) \approx \sin^2\left(\frac{\pi}{2}\frac{z}{l_{coh}}\right) + m^2 F \sin^2\left(\pi\frac{z}{l_{coh}}\right). \qquad (22)$$

The expressions for the intensity and the NPS of the fundamental waves are derived in [36] for the case of Type II SHG.

This approximation describes (with less than 10% deviation) the amplitude and the phase of interacting waves in quadratic processes as Type I SHG, Type II SHG, sum frequency generation interactions and others. It explains both the disperse like shape of the NPS & $\Delta kL$ dependence (fig. 26.a) and stepwise behaviour of NPS & input amplitude (fig. 26.b) and NPS & distance dependencies.

**7. Conclusion**

In this article we have given a brief review of quadratic cascade processes and of based on these processes nonlinear optical devices, suitable for control laser light parameters. It was shown that $\chi^{(2)}:\chi^{(2)}$ cascading can be used for construction of intensity induced polarization rotators, polarization interferometers with self induced transparency and darkening and intracavity mode-locking devices.

We would like to acknowledge Prof. G. Stegeman, Prof. A. Boardman, Prof. M Fejer, Prof. G. Assanto, Prof. A. P. Sukhorukov and Prof. C. Fabre for the discussions we had during the school. We thank Ch. Iglev and P. Tzankov for their contribution in the works used for writing this review. Bulgarian Science Foundation is also acknowledged for the support via the grants F405 and MUF01.

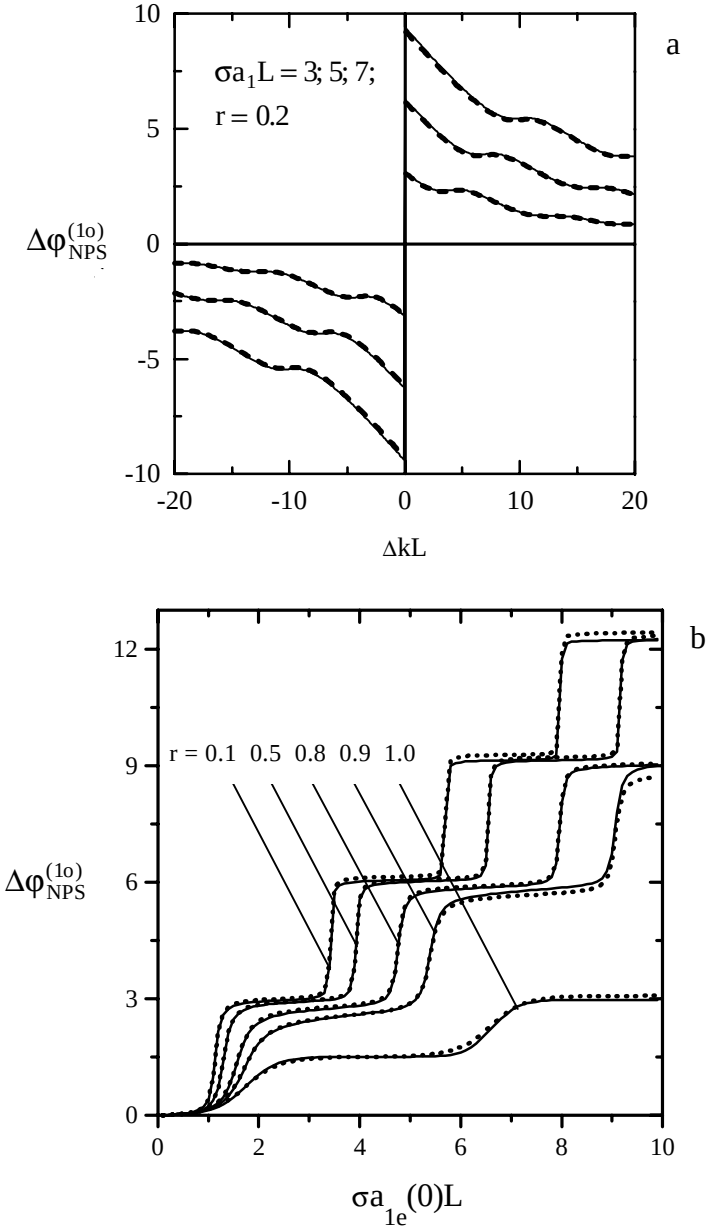


*Figure 26*. Comparison of exact numerical calculations (dotted line) and calculations with high depletion approximation (solid line) for Type II SHG without seeding.

## 8. References


1. Ippen, E. and Shank, C. (1977) Techniques for measurement, in S. Shapiro (ed.), Ultrashort Light Pulses-Picosecond Techniques and Applications, Springer-Verlag, Berlin, p. 83.
2. Giordmaine, J.,Rentzepis, P., Shapiro, S. and Wecht, K. (1967) Two-photon excitation of fluorescence by picosecond light pulses, *Appl. Phys. Lett.* **11**, 216-218.
3. Saltiel, S., Stankov, K., Yankov, P. and Telegin, V. (1986) Realization of a diffraction grating autocorrelator for single-shot ultra short light pulse measurements, *Appl. Phys. B* **40**, 25-27.
4. Kurobori, T., Cho, Y., Matsuo, Y. (1981) An intensity phase autocorrelator for the use of ultrashort pulse measurements, *Opt. Commun*. **40**, 156-60.
5. Diels, J., Fontaine, J, McMichael, I and Simoni, F. (1985) Control and measurement of ultrashort pulse shapes (in amplitude and phase) with femtosecond accuracy, *Appl. Opt*. **24**, 1270-1282.
6. Walmsley, I. and Trebino, R. (1996) Measuring Fast Pulses, *Optics & Photonics News*, No3., 24-33.
7. Delong, K., Trebino, R., Hunter, J. and White, W. (1994) Frequency resolved optical gating with the use of second harmonic generation, *JOSA B* **11**, 2206-2215.
8. Delong K., Fittinghof, D. and Trebino, R. (1996) Practical Issues in Ultrashort-Laser-Pulse Measurement Using Frequency-Resolved Optical Gating, *IEEE J. Quant. Electr*. **32**, 1253-1264.
9. Sullivan, A., White, W., Chu, K., Herritage, J., Delong, K. and Trebino, R. (1996) Quantitative investigation of optical phase matched techniques for ultrashort pulse lasers, *JOSA B* **13**, 1965-1978.
10. Saltiel, S., Yankov, P. and Zheludev, N. (1987) Second harmonic generation as a method for polarizing and analysing laser light, *Appl.Phys. B*, **42**, 115-119.
11. Zheludev, N., Saltiel, S. and Yankov, P. (1987) Second Harmonic Devices - a new class polarizers and analysers, *Sov.J.Quantum Electron*. **17**, 948-952.
12. Stankov, K. (1988)A Mirror with an Intensity Dependent Reflection Coefficient, *Applied Physics B* **45**, 191-194.
13. Stankov K. and Jethwa, J. (1988) A new mode-locking technique using non-linear mirror, *Opt. Commun*. **66**, 41-44.
14. Stankov, K., Kubecek, V., Hamal, K. (1991) Mode locking of a laser at the 1.34 μm transition by a second harmonic non-linear mirror, *Opt. Lett.* **16**, 505-507.
15. Danailov, M., Cerullo, G., Magni, V., Segala, D., De Silvestri, S. (1994) Non-linear mirror mode locking of a CW Nd:YLF laser, *Opt. Lett*. **19**, 792-794.
16. Buchvarov, I., Saltiel, S., Gagarski, S. (1995) on-linear doubling mode-locking of feedback controlled pulsed Nd:YAG laser, *Opt.Commun*. **118**, 51-54.
17. Cerullo, G.,. De Silvestri, S., Monguzzi, A., Segala D. and Magni V. (1995) Self-starting mode locking of a CW Nd:YAG laser using cascaded second order nonlinearities, *Opt. Lett.* **20**, 746-748.
18. Buchvarov, I., Stankov, K., Saltiel, S., Georgiev, D. (1991) Pulse shortening in an actively mode locked laser with frequency doubling nonlinear mirror, *Opt. Commun*. **83**, 241-245.
19. Buchvarov, I., Saltiel, S., Stankov, K., Georgiev, D. (1991) Extremely long train of ultra short pulses from an actively mode locked pulsed Nd:YAG laser, *Opt. Commun*. **83**, 65-70.
20. Stankov, K. (1991) negative feedback uding a nonlinear mirror for the generation of a long train of short light pulses, *Appl. Phys. B* **52**, 158-162.
21. De Salvo, R., Hagan, D., Sheik Bahae, M., Stegeman, G., Van Stryland, E. (1992) Self-focusing and self-defocusing by cascaded second order effects in KTP, *Opt. Lett*. **17**, 28-30.
22. Stegeman, G., Sheik-Bahae, M., Van Stryland, E., Assanto, G. (1993) Large nonlinear phase shift in second-order nonlinear optical processes, *Opt. Lett*. **18**, 13-15.
23. Assanto, G., Stegeman, G., Sheik-Bahae, M., Van Stryland, E. (1995) Coherent interactions for all-optical signal processing via quadratic nonlinearities, *IEEE J.Quant.Electron*, **31**, 673-681.
24. Stegeman, G., Hagan, D. and Torner, L. (1996) $\chi^{(2)}$ cascading phenomena and their applications to all-optical signal processing, mode-locking, pulse compression and solitons, *J. Opt.&Quantum Electron*. **28**, 1691-1740.
25. Stegeman, G., Scheik, R., Torner, L., Torruellas, W., Baek, Y., Baboiu, D., Wang, Z., Van Stryland E., Hagan, D. and Assanto, G (199) Cascading: a promising approach to nonlinear optical phenomena, in *Novel Optical Materials and Applications* ed. by I-C. Khoo F. Simoni and C. Umeton (JOHN WILEY&SONS, INC), pp. 49-76.
26. Hutchings, D., Aitchison, J., Ironside, C. (1993) All-optical switching based on nondegenerate phase shifts from a cascaded second-order nonlinearity, *Opt.Lett*. **18**, 793-795.
27. Belostotsky, A., Leonov, A., Meleshko, A. (1994) Nonlinear phase change in type II second harmonic generation under exact phase-matched conditions, *Opt.Lett*. **19**, 856-858.
28. Assanto, G. and Torelli, I. (1995) Cascading effects in type II second harmonic generation: applications to all-optical processing, *Opt. Commun*. **119**, 143-148.
29. Assanto, G., Wang, Z., Hagan, D. and VanStryland, E. (1995) All-optical modulation via nonlinear cascading in type II second harmonic generation, *Appl. Phys. Lett*. **67,** 2120-2122..
30. Saltiel, S., Koynov, K., Buchvarov, I. (1995) Analytical and numerical investigation of opto-optical phase modulation based on coupled second order nonlinear processes, *Bulg. J. Phys*. **22** 39-47.

31. Saltiel, S., Koynov, K., Buchvarov, I. (1996), Analytical formulae for optimisation of the process of lower phase modulation in a quadratic nonlinear medium, *Appl. Phys. B* **62**, 39-42.
32. Hagan, J., Sheik-Bahae, M., Wang, Z., Stegeman, G., Van Stryland, E., Assanto, G. (1994) Phase controlled transistor action by cascading of second order nonlinearities *Opt. Lett*. **19**, 1305-1307.
33. Assanto, G., Torelli, I. and Trillo, S. (1994) All-optical processing by means of vectorial interactions in second-order cascading: novel approaches, *Opt. Lett*., **19**, 1720-1722.
34. Saltiel, S., Koynov, K., Buchvarov, I. (1996) Self-induced transparency and self-induced darkening with nonlinear frequency doubling polarization interferometer, *Appl. Phys. B* **63**, 371-374.
35. Lefort, L. and Barthelemy, A. (1995) Intensity dependent polarization rotation associated with type II phase-matched second-harmonic generation: application to self-induced transparency, *Opt. Lett*. **20** 1749-1751.
36. Buchvarov, I., Saltiel, S., Iglev, Ch., Koynov, K. (1997) Intensity dependent change of the polarization state as a result of non-linear phase shift in type II frequency doubling crystals, *Opt. Commun*. **141**, 173-179.
37. Akhmanov, S. and Khokhlov, R. Problems of Nonlinear Optics, Moscow: Acad. Nauk SSR (1964), English ed. New York: Gordon&Breach.
38. Yablonovitch, E., Flytzanis, C. and Blombergen, N., Anisotropic (1972) Interference of Three Wave Frequency Mixing in GaAs, *Phys. Rev. Lett*. **29** 865-868.
39. Akhmanov, S., Meysner, L., Parinov, S., Saltiel, S., Tunkin, V. (1977) Third Order Nonlinear Optical Susceptibilities of Crystals; Signs and amplitudes of the Susceptibilities in Crystals with and without Inversion Center, *Sov. Phys. JETP* **46**, 898-907.
40. Pfister, O., Wells, J., Hollberg, L., Zink, L., Van Baak, D., Levenson, M., Basenberg, W. (1997) Continuous-wave frequency tripling and quadrupling by simultaneous three wave mixings in periodically poled crystals: application to a two-step 1.19-10.71 μm frequency bridge, *Opt. Lett*. **22**, 1211-1213.
41. Koynov, K., Saltiel, S. and Buchvarov, I. (1997) All-optical switching by means of interferometer with nonlinear frequency doubling mirrors", *JOSA B* **14**, 830-834.
42. Tagiev, Z., Chirkin, A. (1977) Fixed Intensity Approximation in Wave Theory, *ZETPh* **73,** 1271-1281, (in Russian).
43. Saltiel, S., Koynov, K., Tzankov, P., Boardman, A., Tanev, S. (1998) Nonlinear phase shift as a result of cascaded third-order processes, *Phys Rev A*
44. Koynov, K. and Saltiel, S. (1998) Nonlinear phase shift via multistep $\chi^{(2)}$ cascading, *Opt. Commun.*
45. Asobe, M., Yokohama, I., Itoh, H., Kaino, T. (1997) All-optical switching by use of cascading of phase-matched SFG and DFG processes in periodically poled $LiNbO_3$, *Opt. Lett*. **22**, 274-276.
46. Kobyakov, A., Lederer, F. (1996) Cascading of quadratic nonlinearities: an analytical study, *Phys. Rev. A*, **54**, 3455-3471.
47. Cerullo, G., Danailov, M., De Silvestri, S., Laporta, P., Monguzzi, A., Magni, V., Segala, D. and Taccheo, T. (1994) A diode pumped nonlinear mirror mode-locked Nd:YAG laser, *Appl. Phys. Lett*. **65**, 2392-2394.
48. Stankov, K. (1991) 25 ps pulses from a Nd:YAG laser lode-locked by a frequency doubling β-$BaB_2O_4$ crystal, *Appl. Phys. Lett*. **58**, 2203-2206.
49. Barr, J. and Hughes, D. (1989) Coupled cavity mode-locking of a ND:YAG laser using second-harmonic generation, *Appl. Phys. B* **49**, 323-325.
50. Buchvarov, I., Saltiel, S., Gagarskii, S. (1995) Nonlinear Doubling Mode-Locking of Feed-back Controlled Nd:YAG Laser, *Opt. Commun*. **118**, 51-54.
51. Wu, Q., Zhou, J., Huang, X, Li, Z., Li, Q. (1993) Mode-locking with linear and nonlinear phase shifts, *JOSA B*. **10**, 2080-2084.

.